Received: 28 June 2021 | Accepted: 10 September 2021

DOI: 10.1002/pros.24239

ORIGINAL ARTICLE

The Prostate WILEY

Characteristics of α2,3-sialyl *N*-glycosylated PSA as a biomarker for clinically significant prostate cancer in men with elevated PSA level

Tohru Yoneyama PhD[1] | Hayato Yamamoto MD, PhD[2] | Mihoko Sutoh Yoneyama PhD[3] | Yuki Tobisawa PhD[2] | Shingo Hatakeyama MD, PhD[2,4] | Takuma Narita MD, PhD[2,5] | Hirotake Kodama MD, PhD[2,6] | Masaki Momota MD, PhD[2,7] | Hiroyuki Ito MD[8] | Shintaro Narita MD, PhD[9] | Fumiyasu Tsushima MD, PhD[10] | Koji Mitsuzuka MD, PhD[11] | Takahiro Yoneyama MD, PhD[2] | Yasuhiro Hashimoto MD, PhD[2] | Wilhelmina Duivenvoorden MD, PhD[12] | Jehonathan H. Pinthus MD, PhD[12] | Shingo Kakeda MD, PhD[10] | Akihiro Ito MD, PhD[11] | Norihiko Tsuchiya MD, PhD[13] | Tomonori Habuchi MD, PhD[9] | Chikara Ohyama MD, PhD[2,4]

[1]Department of Glycotechnology, Center for Advanced Medical Research, Hirosaki University Graduate School of Medicine, Hirosaki, Aomori, Japan

[2]Department of Urology, Hirosaki University Graduate School of Medicine, Hirosaki, Aomori, Japan

[3]Department of Cancer Immunology and Cell Biology, Oyokyo Kidney Research Institute, 90 Yamazaki Kozawa, Hirosaki, Aomori, Japan

[4]Department of Advanced Blood Purification Therapy, Hirosaki University Graduate School of Medicine, Hirosaki, Aomori, Japan

[5]Department of Urology, National Hospital Organization Hirosaki National Hospital, Hirosaki, Aomori, Japan

[6]Department of Urology, Tsugaru General Hospital, Goshogawara, Aomori, Japan

[7]Department of Urology, Mutsu General Hospital, Mutsu, Aomori, Japan

[8]Department of Urology, Aomori Rosai Hospital, Hachinohe, Aomori, Japan

Abstract

Background: The presence of glycosylated isoforms of prostate-specific antigen (PSA) in prostate cancer (PC) cells is a potential marker of their aggressiveness. We characterized the origin of α2,3-sialylated prostate-specific antigen (S23PSA) by tissue-based sialylation-related gene expression and studied the performance of S23PSA density (S23PSAD) alone and in combination with multiparametric magnetic resonance imaging (MRI) for the detection of clinically significant prostate cancer in men with elevated PSA.

Methods: Tissue-based quantification of S23PSA and sialyltransferase and sialidase gene expression was evaluated in 71 radical prostatectomy specimens. The diagnostic performance of S23PSAD was studied in 1099 men retrospectively enrolled in a multicenter systematic biopsy (SBx) cohort. We correlated the S23PSAD with Prostate Imaging Reporting and Data System (PI-RADS) scores in 98 men prospectively enrolled in a single-center MRI-targeted biopsy (MRI–TBx) cohort. The primary outcome was the PC-diagnostic performance of the S23PSAD, the secondary outcome was the avoidable biopsy rate of S23PSAD combined with DRE and total PSA (tPSA), and with or without PI-RADS.

Tohru Yoneyama and Hayato Yamamoto equally contributed authors.

[9]Department of Urology, Akita University Graduate School of Medicine, Akita, Japan

[10]Department of Radiology, Hirosaki University Graduate School of Medicine, Hirosaki, Aomori, Japan

[11]Department of Urology, Tohoku University Graduate School of Medicine, Sendai, Miyagi, Japan

[12]Department of Surgery, McMaster University, Hamilton, Ontario, Canada

[13]Department of Urology, Yamagata University Faculty of Medicine, Yamagata, Japan

Correspondence

Tohru Yoneyama, Department of Glycotechnology, Center for Advanced Medical Research, Hirosaki University Graduate School of Medicine, 5 Zaifu-cho, Hirosaki, 036-8562 Aomori, Japan.
Email: tohruyon@hirosaki-u.ac.jp

Chikara Ohyama, Department of Urology, Hirosaki University Graduate School of Medicine, 5 Zaifu-cho, Hirosaki 036-8562, Japan.
Email: coyama@hirosaki-u.ac.jp

Funding information

Sakurai Memorial Medical Research Foundation; Japan Society for the Promotion of Science, Grant/Award Numbers: 15H02563, 15K15579

Results: S23PSA was significantly higher in Gleason pattern 4 and 5 compared with benign prostate tissue. In the retrospective cohort, the performance of S23PSAD for detecting PC was superior to tPSA or PSA density (PSAD) (AUC: 0.7758 vs. 0.6360 and 0.7509, respectively). In the prospective cohort, S23PSAD was superior to tPSA, PSAD, and PI-RADS (AUC: 0.7725 vs. 0.5901, 0.7439 and 0.7305, respectively), and S23PSAD + PI-RADS + DRE + tPSA was superior to DRE + tPSA+PI-RADS with avoidance rate of MRI–TBx (13% vs. 1%) at 30% risk threshold.

Conclusions: The diagnostic performance of S23PSAD was superior to conventional strategies but comparable to mpMRI.

KEYWORDS

biomarker, mpMRI, *N*-glycan, PI-RADS, prostate cancer, PSA, sialylation

1 | INTRODUCTION

Prostate-specific antigen (PSA) is widely used in prostate cancer (PC) screening, but often also leads to prostate biopsies, overdiagnosis, and overtreatment of indolent PC due to the low specificity for the detection of clinically significant PC.[1,2] Multiparametric magnetic resonance imaging (mpMRI) and/or biomarkers (i.e., 4Kscore, SelectMDx, PHI, PCA3, EPI, risk calculators, and aberrantly glycosylated PSAs) are used for risk stratification of men with relatively low PSA and normal DRE before recommending systematic prostate biopsy (SBx).[3–12] We focused on the ratio of PC-associated nonreducing terminal α2,3-sialylated PSA (S23PSA) in serum, in relation to α2,6-sialylated PSA (S26PSA) which is exclusive to benign prostate and established automated microfluidic technology-based simultaneous immunoassay system.[13,14] We recently reported that the diagnostic performance of S23PSA (area under the curve (AUC, 0.8340)) outperforms that of tPSA (AUC, 0.5062).[10] In this study, we investigated the origin of S23PSA by tissue-based quantification of S23PSA and sialylation-related gene expression, and also evaluated the clinical significance of S23PSA density (S23PSAD) in a multicenter retrospective SBx cohort and a single-center prospective MRI-targeted ultrasound-guided prostate biopsy (MRI–TBx) cohort.

2 | MATERIALS AND METHODS

2.1 | Study design and assessments

The flow diagram of this study is shown in Figure 1. S23PSA level and sialylation-related gene expression in benign and tumor prostate tissues were evaluated in 71 patients who underwent radical prostatectomy at Hirosaki University between January 2016 and January 2017. The diagnostic performance of S23PSA and S23PSAD in determining PC and High grade PC (HGPC) at the initial SBx was retrospectively evaluated in the SBx cohort ($n = 1099$) in patients from Hirosaki University and five related hospitals, Akita University, Yamagata University, Tohoku University in Japan, and McMaster University in Canada between June 2010 and January 2020. The correlation between prebiopsy S23PSA value, Prostate Imaging Reporting and Data System (PI-RADS),[15] and MRI–TBx outcome was also prospectively evaluated in MRI–TBx cohort which enrolled 98 men suspected with PC due to elevated PSA > 4 ng/ml and/or abnormal DRE findings and who underwent both SBx and MRI–TBx at Hirosaki University between January 2018 and January 2021. Eligible participants comprised men with PSA ≤ 50 ng/ml who received SBx. Men with N1 or M1 PC or Men with a history of invasive treatment for prostatic hyperplasia or who were

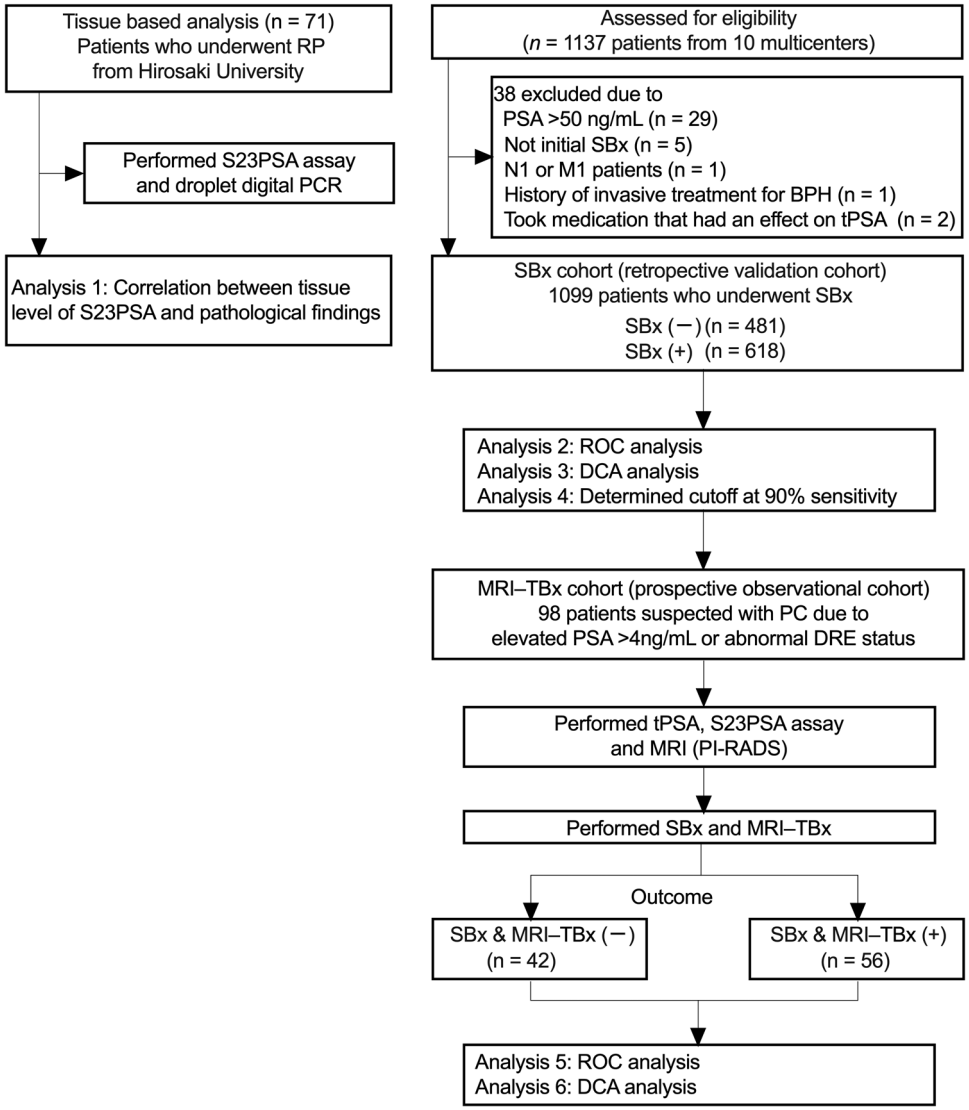

FIGURE 1 A flow diagram of the studies. A tissue-based analysis was evaluated in 71 patients who underwent radical prostatectomy at Hirosaki University. The correlation between tissue S23PSA ratio and sialylation-related gene expression and pathological findings were evaluated (Analysis 1). All samples were subjected to S23PSA assay and droplet digital PCR analysis. A retrospective SBx cohort enrolled 1099 patients with SBx(–) (n = 481) and SBx(+) (n = 618) men who underwent SBx at 10 institutions between June 2010 and January 2020. All sera were subjected to S23PSA, S23PSAD, tPSA, F/T PSA, and PSAD assays. The PC or HGPC diagnostic performances of each assay were compared using ROC analysis (Analysis 2). The clinical impacts of adding the F/T PSA, PSAD, S23PSA, and S23PSAD to the DRE status and tPSA were evaluated using DCA (Analysis 3). The cutoff value of each assay at 90% sensitivity was determined (Analysis 4). A prospective observational cohort enrolled 98 patients who were suspected with PC due to elevated PSA or abnormal DRE status at a single institution between January 2018 and January 2020. All sera were subjected to S23PSA, S23PSAD, PSAD, and tPSA assays before SBx and MRI–TBx. The PC or HGPC diagnostic performances of each assay using the cutoff value defined by the retrospective SBx cohort were compared using ROC analysis (Analysis 5). The clinical impact of adding the PI-RADS, PSAD, S23PSA, and S23PSAD to the DRE status and tPSA was evaluated using DCA (Analysis 6). DCA, decision curve analyses; DRE, digital rectal examination; MRI, magnetic resonance imaging; PCR, polymerase chain reaction; PSA, prostate-specific antigen; RP, radical prostatectomy; ROC, receiver operating characteristic curve

taking medication effecting tPSA levels 6 months before serum collection were excluded. All sera were collected before biopsy and stored at −80°C until use. The grade group (GG) according to the International Society of Urological Pathology guideline[16] for Bx specimens was assessed by histopathologists at each institution blinded to each patient's S23PSA value. HGPC was defined as greater than GG2. This study was conducted in accordance with the ethical standards of the Declaration of Helsinki and was approved by the ethics committee of each institution (approval number, 2019–055, https://www.med.hirosaki-u.ac.jp/hospital/outline/resarch/resarch.html). Written informed consent was obtained from all patients.

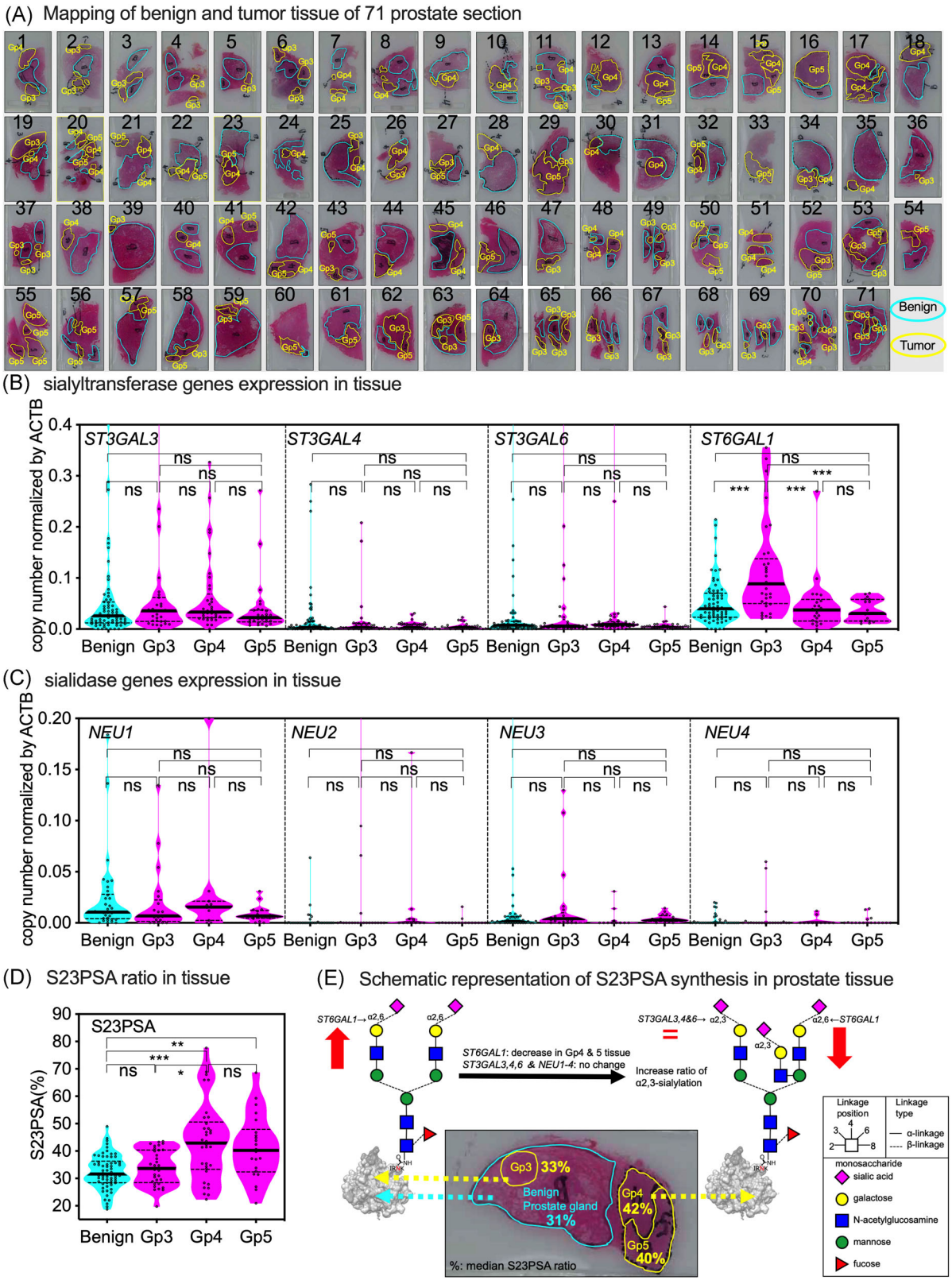

FIGURE 2 (See caption on next page)

2.2 | Determination of S23PSA and S23PSAD

S23PSA (expressed as ratio [%] of S23PSA over [S23PSA + S26PSA]) was measured using an automated microfluidic technology-based simultaneous immunoassay as previously described.[10] S23PSAD (%/cm^3) was calculated by dividing the S23PSA value by the prostate volume measured using transrectal ultrasonography (TRUS) prostate ellipse volume calculation (height × length × width × π/6). tPSA and free PSA were measured using ECLusys total PSA and free PSA on Covas 8000/e 801 (Roche Diagnostics K.K). PSA density (PSAD, ng/ml/cm^3) was calculated by dividing the tPSA value by the prostate volume measured using TRUS. All assays of retrospective samples were conducted within 2 years after serum collection. Duplicate assays were used for each sample.

2.3 | Quantification of sialyltransferases and sialidase gene expression in formalin-fixed paraffin-embedded (FFPE) prostate tissue

Tissue extracts and total RNA from benign and tumor tissues prepared from macro-dissected 20-μm thick FFPE prostate sections (Figure 2A). cDNA synthesis and droplet digital PCR (ddPCR) analysis were performed as previously described.[9] The ddPCR probes for each gene were purchased from Bio-Rad Laboratories and were as follows: Human α2,3-sialyltransferase 3 (*ST3GAL3*) (ID: dHsaCPE5029784), α2,3-sialyltransferase 4 (*ST3GAL4*) (ID: dHsaCPE5050730), α2,3-sialyltransferase 6 (*ST3GAL6*) (ID: dHsaCPE5032628), α2,6-sialyltransferase 1 (*ST6GAL1*) (ID: dHsaCPE5030930), sialidase 1 (*NEU1*) (ID: dHsaCPE5190611), sialidase 2 (*NEU2*) (ID: dHsaCPE5035070), sialidase 3 (*NEU3*) (ID: dHsaCPE5039204), sialidase 4 (*NEU4*) (ID: dHsaCPE5029056), and β-actin (*ACTB*) (ID: dHsaCPE5190200). The absolute copy number of *ST3GAL3*, *4*, *6*, *ST6GAL1*, and *NEU1–4* genes were normalized to the ACTB. Triplicate assays were used for each sample.

2.4 | Systematic prostate biopsy in retrospective study and mpMRI targeted prostate biopsy in a prospective study

TRUS-guided SBx (10 cores) was performed by experienced urologists in a retrospective study. In a prospective study, all MRI examinations were performed at 3.0 Tesla using a pelvic phased-array coil, including T2-weighted imaging and diffusion-weighted imaging with apparent diffusion coefficient mapping. Target lesions for MRI-ultrasonography fusion-guided biopsy were chosen in a clinical setting by experienced radiologists who had access to feedback through pathological results. Index lesions were scored according to PI-RADS ver.2.[15] Targeted biopsy with SBx was performed using the BioJet™ fusion system (D&K Technologies) and a Prosound α7 (Hitachi Aloka Medical) combined with TRUS transperineal biopsy platform. The segmentation into a two-dimensional mpMRI was performed on a workstation to create a three-dimensional MRI model and fused to real-time TRUS using elastic fusion. The biopsy process started with targeted biopsies which were performed for lesions with PI-RADS ver.2 categories of 1–5, and at least two cores were taken for MRI-targeted lesions, and then systematic Bx (n = 12) was performed transperineally by experienced urologists. An 18-G biopsy gun with a 22-mm specimen size (Primcut II; Boston Scientific Japan) was used to perform the biopsies.

2.5 | Statistical analyses

All statistical calculations were performed using Graphpad Prism 8 (GraphPad), STATA/SE15.1 (StataCorp LLC). For the non-normally distributed model, the Mann–Whitney U test and the Kruskal–Wallis test were used to analyze intergroup and multigroup differences, respectively. The correlation analysis was analyzed using the non-parametric Spearman rank-order correlation test. Predictive accuracy was quantified as AUC of the receiver operating characteristic curves. The clinical net benefit of the diagnostic standard of care, which included tPSA and DRE status, with and without F/T PSA, PSAD, S23PSA, S23PSAD, PI-RADS for predicting PC, and HGPC was evaluated using the decision curve analysis (DCA) that was developed using the rmda package of R version 3.5.2 (R Foundation for Statistical Computing; http//www.r-project.org/).[17] P values of less than 0.05 were used to denote statistical significance.

3 | RESULTS

3.1 | Tissue-based quantification of S23PSA and sialyltransferase and sialidase gene expression

To characterize the origin of S23PSA, we determined the ratio of S23PSA and expression of α2,6- or α2,3- sialyltransferases and sialidases genes in prostate tissue. Nonreducing terminal sialylation

FIGURE 2 Ratio of S23PSA and sialyltransferases and sialidases gene expression in formalin-fixed paraffin-embedded (FFPE) prostate benign and tumor tissues. (A) Total RNA and total protein were extracted from benign tissue, and each Gleason pattern (Gp) of tumor tissue macrodissected from 20-μm-thick FFPE prostate sections indicated by the areas marked with *solid yellow* and *dashed outline*, respectively. (B) and (C) The levels of *ST3GAL3*, *4*, *6*, *ST6GAL1*, and *NEU1*, *2*, *3*, *4* gene expression in benign and tumor tissues with Gp3–5. (D) The ratio of the S23PSA in benign and tumor tissues with Gp3–5. The *dashed black line* in the violin plots outlines the interquartile range (IQR). The *solid bold black line* represents the median value. *ns* not significant; *p < 0.05, **p < 0.005, ***p < 0.0005. (E) Schematic representation of S23PSA synthesis in prostate tissue [Color figure can be viewed at wileyonlinelibrary.com]

TABLE 1 Characteristics of SBx cohort

Total (*n* = 1099)	**SBx(−) (*n* = 481)**	**SBx(+) (*n* = 618)**	
Variables	Median (IQR)	Median (IQR)	*p*[a]
Age at SBx	68 (62–73)	69 (65–73)	0.0008
DRE normal/nodule+	446/35	319/299	<0.0001
Prostate volume, cm^3	38.92 (27.85–52.17)	27.80 (21.00–38.00)	<0.0001
tPSA, ng/ml	6.14 (4.51–8.99)	7.38 (5.13–11.68)	<0.0001
F/T PSA, %	21.34 (15.35–31.47)	14.48 (10.21–20.73)	<0.0001
PSAD, ng/ml/cm^3	0.162 (0.104–0.244)	0.269 (0.169–0.472)	<0.0001
S23PSA, %	42.20 (35.50–48.55)	51.95 (44.80–59.13)	<0.0001
S23PSAD, %/cm^3	1.03 (0.71–1.56)	1.94 (1.28–2.60)	<0.0001
Clinical stage		*n* (%)	
1c		316 (51.1)	
2a		140 (22.7)	
2b		52 (8.4)	
2c		44 (7.1)	
3		62 (10.0)	
4		4 (0.6)	
SBx GG		*n* (%)	
GG 1		118 (19.1)	
GG 2		190 (30.7)	
GG 3		104 (16.8)	
GG 4		87 (14.1)	
GG 5		119 (19.3)	
Subgroup with tPSA levels ranging from 4–10 ng/ml			
(*n* = 654)	SBx(−) (*n* = 299)	SBx(+) (*n* = 355)	*p*[a]
Age (years)	67 (62–73)	68 (65–73)	0.0144
DRE normal/nodule+	279/20	199/156	<0.0001
Prostate volume, cm^3	38.42 (28.00–53.00)	28.00 (20.41–39.00)	<0.0001
tPSA, ng/ml	6.09 (5.00–7.47)	6.21 (5.06–7.76)	>0.9999
F/T PSA, %	20.05 (15.00–29.85)	14.39 (10.80–20.31)	<0.0001
PSAD, ng/ml/cm^3	0.165 (0.112–0.221)	0.224 (0.160–0.308)	<0.0001
S23PSA, %	42.40 (35.50–49.30)	50.60 (43.90–57.90)	<0.0001
S23PSAD, %/cm^3	1.03 (0.73–1.56)	1.88 (1.19–2.61)	<0.0001
Clinical stage		*n* (%)	
1c		198 (55.8)	
2a		88 (24.8)	
2b		25 (7.0)	
2c		27 (7.6)	
3		15 (4.2)	
4		2 (0.6)	

Total (n = 1099)	SBx(−) (n = 481)	SBx(+) (n = 618)
SBx GG		n (%)
GG 1		71 (20.0)
GG 2		130 (36.6)
GG 3		63 (17.7)
GG 4		48 (13.5)
GG 5		43 (12.1)

Abbreviations: DRE, digital rectal examination; F/T PSA, free PSA/tPSA; GG, grade group; IQR, interquartile range; PSAD, tPSA density; SBx, systematic prostate biopsy; S23PSA, α2,3-sialylated prostate-specific antigen ratio; S23PSAD, S23PSA density; tPSA, total PSA.
[a]Mann–Whitney U test.

of *N*-glycan is regulated by a balance between sialyltransferases and sialidases expression.[18,19] The expression of α2,6-sialylation-related *ST6GAL1* gene in Gp4 (median 0.038, interquartile range (IQR), 0.016–0.058) and 5 (0.031, IQR 0.016–0.058) tissues was significantly decreased compared to Gp3 (0.089, IQR 0.050–0.138) tissue and comparable to benign prostate gland (0.040, IQR 0.023–0.070). However, no significant changes in the expression levels of α2,3-sialylation-related *ST3GAL3*, *4*, *6* and sialidase *NEU1–4* genes were noted between the benign and tumor tissues (Figure 2A–C). Consequently, the S23PSA ratio was significantly increased in Gp4 (median 42.87%, IQR 33.27%–50.51%) and 5 (40.22%, IQR 32.36%–47.94%) tissues compared with benign prostate gland (31.59%, IQR 28.41%–36.33%) and Gp3 (33.67%, IQR 28.48%–40.36%) tissue (Figure 2D).

3.2 | Diagnostic performance of each assay in the retrospective SBx cohort

The characteristics of the retrospective SBx cohort (n = 1099) are shown in Table 1. Of those with PC (n = 618), 118 cases were classified as GG1, the remaining 500 cases as HGPC. Among HGPC, 190 (30.7%), 104 (16.8%), 87 (14.1%), and 119 (19.3%) were classified as GG2, GG3, GG4, and GG5, respectively. Significant differences in age and DRE status were observed between men with negative SBx and men with positive SBx (p = 0.0008 and p < 0.0001, respectively). In addition, significant differences in prostate volume, and the levels of tPSA, F/T PSA, PSAD, S23PSA, and S23PSAD were found between these two groups (p < 0.0001) (Figure 3A).

The performance of S23PSAD for predicting PC (AUC: 0.7578; 95% confidence interval [CI], 0.7292–0.7864) was significantly better than PSAD (0.7111; 95% CI, 0.6810–0.7412) (p = 0.0017), F/T PSA (0.6978; 95% CI, 0.6666–0.7290) (p = 0.0012), and tPSA (0.6013; 95% CI, 0.5879–0.6347) (p < 0.0001) and comparable to S23PSA (0.7552; 95% CI, 0.7268–0.7836) (p = 0.8369) (Figure 3C). The AUC of S23PSAD for discriminating HGPC (0.7758; 95% CI, 0.7484–0.8032) was significantly higher than of F/T PSA (0.7012; 95% CI, 0.6705–0.7319) (p < 0.0001), tPSA (0.6360; 95% CI, 0.6034–0.6687) (p < 0.0001), and PSAD (0.7509; 95% CI, 0.7222–0.7796) (p = 0.0757) and comparable with S23PSA (0.7651; 95% CI, 0.7374–0.7927) (p = 0.4010) (Figure 3C). At 90% sensitivity, the specificity of S23PSAD (37.2% and 44.9%, respectively) and S23PSA (40.1% and 43.4%, respectively) for detecting PC and HGPC were higher than that of tPSA (18.5% and 22.9%, respectively), F/T PSA (29.1% and 30.1%, respectively), and PSAD (31.2% and 34.7%, respectively) (Table 2).

The characteristics of the SBx cohort belonging to the subgroup of patients with tPSA levels ranging from 4–10 ng/ml (n = 654) are shown in Table 1. Among the 355 patients with PC, 71 were classified as GG1. Of the remaining 284 patients with HGPC, 130 (36.6%), 63 (17.7%), 48 (13.5%), and 43 (12.1%) were classified as GG2, GG3, GG4, and GG5, respectively. No significant difference in the tPSA level was found between men with negative SBx and men with positive SBx (p > 0.9999). Significant differences in age and DRE status were observed between the groups. Significant differences in the levels of prostate volume, F/T PSA, PSAD, S23PSA, and S23PSAD were also found between men with negative SBx and positive SBx (p < 0.0001) (Figure 3B).

S23PSAD (AUC 0.7428; 95% CI, 0.7052–0.7803) provided a significantly better clinical performance for predicting PC than PSAD (0.6793; 95% CI, 0.6385–0.7200) (p < 0.0001), F/T PSA (0.6793; 95% CI, 0.6380–0.7205) (p = 0.0077), and tPSA (0.5168; 95% CI, 0.4724–0.5612) (p < 0.0001), and a clinical performance comparable to that of S23PSA (0.7266; 95% CI, 0.6882–0.7651) (p = 0.3442) (-Figure 3D). S23PSAD (AUC 0.7704; 95% CI, 0.7344–0.8063) also provided a significantly better clinical performance for predicting HGPC than PSAD (0.7140; 95% CI, 0.6745–0.7535) (p < 0.0001), F/T PSA (0.6898; 95% CI, 0.6492–0.7304) (p = 0.0007), and tPSA (0.5431; 95% CI, 0.4984–0.5878) (p < 0.0001) and a clinical performance comparable with that of S23PSA (0.7484; 95% CI, 0.7112–0.7855) (p = 0.1729) (Figure 3D). At a preset 90% sensitivity, the specificity of S23PSAD (36.1% and 41.9%, respectively) and S23PSA (32.4% and 44.9%, respectively) for detecting PC and HGPC was higher than that of tPSA (10.4% and 10.3%, respectively), F/T PSA (27.4% and 28.9%, respectively), and PSAD (25.8% and 31.9%, respectively) (Table 2).

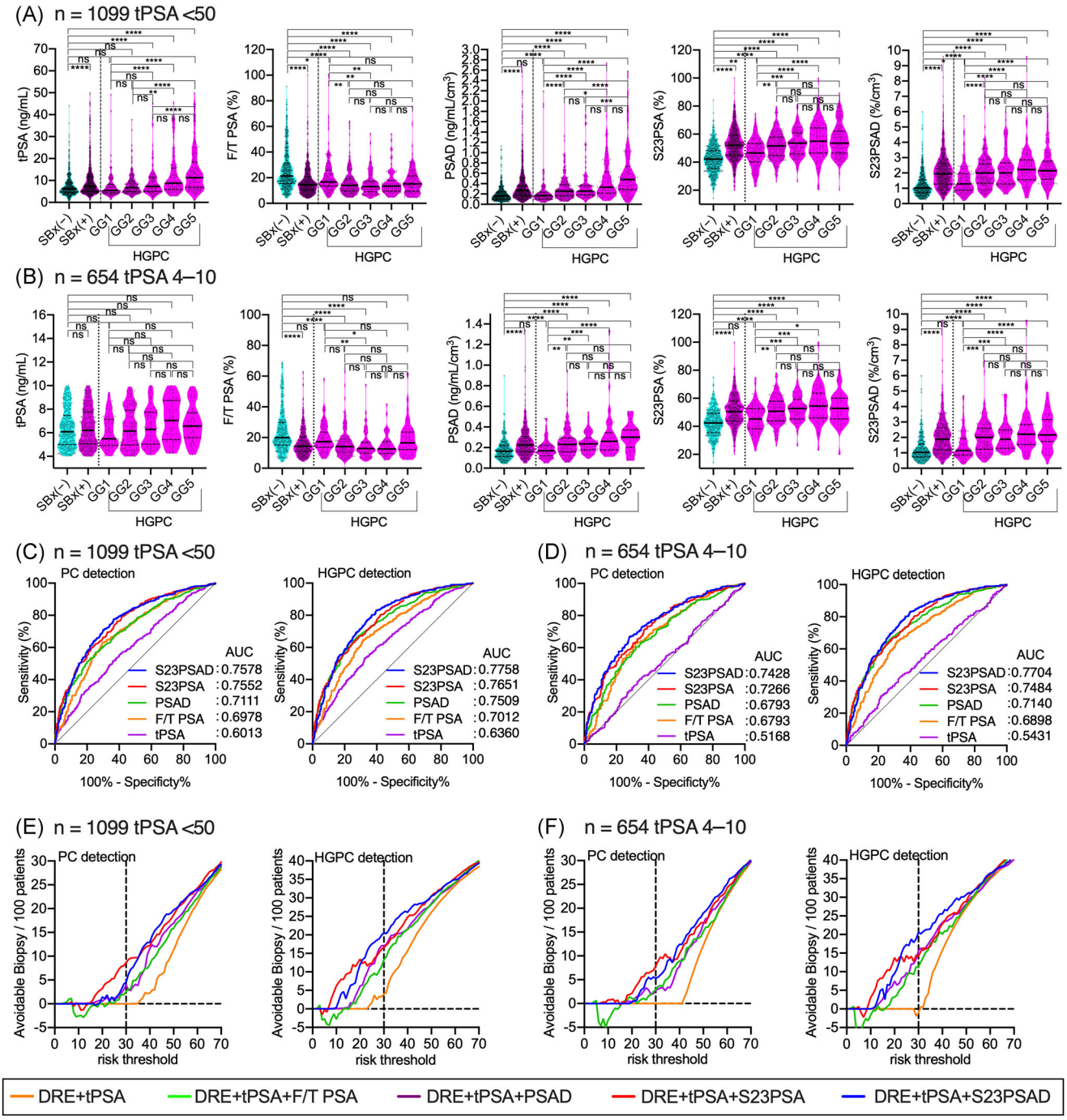

FIGURE 3 Serum levels, ROC and DCA analysis of S23PSA, S23PSAD, tPSA, F/T PSA, and PSAD in the retrospective SBx cohort. (A) and (B) *Violin plot* of each test in the SBx cohort (A) and in the SBx cohort with a tPSA ranging from 4 to 10 ng/ml (B). The SBx(+) group was classified as GG1, and the HGPC group includes GG2, GG3, GG4, and GG5. The *dashed black lines* outline the IQR of each test value. The *solid bold black line* represents the median value of each test value. Multiple group differences were analyzed using the Kruskal–Wallis test for non-normally distributed models. *ns* not significant; $^{*}p < 0.05$, $^{**}p < 0.005$, $^{***}p < 0.0005$, $^{****}p < 0.0001$. (C) and (D) The ROC curves of PC and HGPC prediction accuracy of each assay in the SBx cohort (C) and in the SBx cohort with a tPSA ranging from 4 to 10 ng/ml (D). (E) and (F) Decision curve analysis (DCA) showing net benefit for performing a biopsy in men at risk of PC or HGPC. The number of avoidable biopsies per 100 patients without missing PC or HGPC in the SBx cohort (E) and in the SBx cohort with a tPSA ranging from 4 to 10 ng/ml (F). DCA, decision curve analyses; IQR, interquartile range; PSA, prostate-specific antigen; ROC, receiver operating characteristic curve; tPSA, total PSA [Color figure can be viewed at wileyonlinelibrary.com]

TABLE 2 Specificity at 90% sensitivity of each assay in retrospective SBx cohort

PC detection	tPSA	F/T PSA	PSAD	S23PSA	S23PSAD
Cut-off	>4.025 ng/ml	<29.55%	>0.1165 ng/ml/cm^3	>39.95%	>0.8750%/cm^3
AUC (95%CI)	0.6013 (0.5679–0.6347)	0.6978 (0.6666–0.7290)	0.7111 (0.6810–0.7412)	0.7552 (0.7268–0.7836)	0.7578 (0.7292–0.7864)
p (vs. S23PSAD)	<0.0001	0.0012	0.0017	0.8369	
Specificity, %	18.5	29.1	31.2	40.1	37.2
PPV, %	58.6	62.0	62.7	65.9	64.8
NPV, %	58.9	69.3	70.8	75.7	74.3
FPR, %	81.5	70.9	68.8	59.9	62.8
FNR, %	10.0	10.0	10.0	10.0	10.0
HGPC detection	tPSA	F/T PSA	PSAD	S23PSA	S23PSAD
Cut-off	>4.275 ng/ml	<27.94%	>0.1295 ng/ml/cm^3	>41.45%	>0.9970%/cm^3
AUC (95% CI)	0.6360 (0.6034–0.6687)	0.7012 (0.6705–0.7319)	0.7509 (0.7222–0.7796)	0.7651 (0.7374–0.7927)	0.7758 (0.7484–0.8032)
p (vs. S23PSAD)	<0.0001	<0.0001	0.0757	0.4010	
Specificity, %	22.9	30.1	34.7	43.4	44.9
PPV, %	49.3	51.8	53.5	57.0	57.7
NPV, %	73.3	78.3	80.6	83.9	84.3
FPR, %	77.1	69.9	65.3	56.6	55.1
FNR, %	10.0	10.0	10.0	10.0	10.0
Retrospective SBx cohort (subgroup of patients 4–10 ng/ml tPSA)					
PC detection	tPSA	F/T PSA	PSAD	S23PSA	S23PSAD
Cut-off	>4.493 ng/ml	<28.69%	>0.1125 ng/ml/cm^3	>38.35%	>0.8560%/cm^3
AUC (95%CI)	0.5168 (0.4724–0.5612)	0.6793 (0.6380–0.7205)	0.6793 (0.6385–0.7200)	0.7266 (0.6882–0.7651)	0.7428 (0.7052–0.7803)
p (vs. S23PSAD)	<0.0001	0.0077	<0.0001	0.3242	
Specificity, %	10.4	27.4	25.8	32.4	36.1
PPV, %	54.3	59.5	59.0	61.2	62.5
NPV, %	46.3	69.5	68.1	72.9	75.0
FPR, %	89.6	72.6	74.2	67.6	63.9
FNR, %	10.1	10.1	10.1	10.1	10.1
HGPC detection	tPSA	F/T PSA	PSAD	S23PSA	S23PSAD
Cut-off	>4.493 ng/ml	<27.05%	>0.1250 ng/ml/cm^3	>41.45%	>0.9505%/cm^3
AUC (95%CI)	0.5431 (0.4984–0.5878)	0.6898 (0.6492–0.7304)	0.7140 (0.6745–0.7535)	0.7484 (0.7112–0.7855)	0.7704 (0.7344–0.8063)
p (vs. S23PSAD)	<0.0001	0.0007	<0.0001	0.1729	
Specificity, %	10.3	28.9	31.9	44.9	41.9
PPV, %	43.4	49.2	50.3	55.6	54.3
NPV, %	56.7	78.7	80.3	85.1	84.2
FPR, %	89.7	71.1	68.1	55.1	58.1
FNR, %	10.2	10.2	10.2	10.2	10.2

Abbreviations: AUC, area under the receiver operating characteristics curve; F/T PSA, free PSA/tPSA; FNR, false-negative rate; FPR, false-positive rate; HGPC, high-grade PC; NPV, negative predictive value; PC, prostate cancer; PPV, positive predictive value; PSAD, tPSA density; S23PSA, α2,3-sialylated prostate-specific antigen ratio; S23PSAD, S23PSA density; tPSA, total PSA.

TABLE 3 Characteristics of prospective MRI-targeted biopsy cohort

Total (*n* = 98)	**MRI–TBx (–) (*n* = 42)**	**MRI–TBx (+) (*n* = 56)**	
Variables	Median (IQR)	Median (IQR)	*p*[a]
Age at MRI–TBx	70 (62–73)	71 (66–75)	0.3380
Prior biopsy yes/no	35/7	43/13	0.4261
DRE normal/abnormal	33/9	41/15	0.4221
Prostate volume, cm^3	56.00 (40.98–76.30)	36.40 (27.00–48.68)	0.0005
tPSA, ng/ml	8.25 (5.37–13.73)	9.46 (7.21–15.50)	0.3241
PSAD, ng/ml/cm^3	0.152 (0.104–0.193)	0.272 (0.153–0.497)	0.0001
S23PSA, %	40.80 (29.20–47.85)	46.50 (40.43–60.58)	0.0150
S23PSAD, %/cm^3	0.66 (0.47–1.07)	1.29 (0.87–1.89)	<0.0001
Clinical stage	*n* (%)	*n* (%)	0.0182[b]
1c	33 (78.6)	41 (73.2)	
2a	6 (14.3)	2 (3.6)	
2b	1 (2.4)	2 (3.6)	
2c	1 (2.4)	0 (0)	
3	1 (2.4)	11 (19.6)	
PI-RADS	*n* (%)	*n* (%)	0.0008[b]
1	0 (0.0)	1 (1.9)	
2	2 (4.8)	0 (0.0)	
3	18 (42.9)	4 (7.1)	
4	12 (28.6)	20 (35.7)	
5	10 (23.8)	31 (55.4)	
SBx & MRI–TBx GG		*n* (%)	
GG 1		6 (10.7)	
GG 2		17 (30.4)	
GG 3		5 (8.9)	
GG 4		13 (23.2)	
GG 5		15 (26.8)	
MRI–TBx in subgroup with ≤75 years old and tPSA of ≤50 ng/ml)			
Total (*n* = 79)	MRI–TBx (–) (*n* = 38)	MRI–TBx (+) (*n* = 41)	
Variables	Median (IQR)	Median (IQR)	*p*[a]
Age at MRI–TBx	69 (61–72)	70 (66–73)	>0.9999
Prior biopsy yes/no	32/6	33/8	0.6651
DRE normal/abnormal	30/8	32/9	0.9226
Prostate volume, cm^3	57.50 (40.98–78.73)	37.30 (27.15–48.50)	0.0005
tPSA, ng/ml	8.76 (5.52–13.83)	8.84 (6.26–14.85)	>0.9999
PSAD, ng/ml/cm^3	0.159 (0.104–0.202)	0.229 (0.153–0.407)	0.0033
S23PSA, %	40.8 (29.53–47.53)	47.60 (40.95–61.90)	0.0039
S23PSAD, %/cm^3	0.66 (0.47–1.02)	1.30 (0.90–1.78)	<0.0001
ERSPC RCs, %	23.00(10.75–38.75)	50.00(37.50–66.50)	<0.0001
Clinical stage	*n* (%)	*n* (%)	0.0392[b]

Total (*n* = 98)	MRI–TBx (–) (*n* = 42)	MRI–TBx (+) (*n* = 56)	
1c	30 (78.9)	32 (78.0)	
2a	5 (13.2)	1 (2.4)	
2b	1 (2.6)	0 (0)	
2c	1 (2.6)	0 (0)	
3	1 (2.6)	8 (19.5)	
PI-RADS	*n* (%)	*n* (%)	0.0003[b]
1	0 (0.0)	1 (2.4)	
2	2 (5.3)	0 (0.0)	
3	16 (42.1)	2 (4.9)	
4	11 (28.9)	13 (31.7)	
5	9 (23.7)	25 (61.0)	
SBx & MRI–TBx GG		*n* (%)	
GG 1		5 (12.2)	
GG 2		14 (34.1)	
GG 3		2 (4.9)	
GG 4		9 (22.0)	
GG 5		11 (26.8)	

Abbreviations: AUC, area under the receiver operating characteristics curve; ERSPC RCs, European Randomized Study of Screening for Prostate cancer risk calculators; F/T PSA, free PSA/tPSA; FNR, false-negative rate; FPR, false-positive rate; HGPC, high-grade PC; MRI, magnetic resonance imaging; NPV, negative predictive value; PC, prostate cancer; PPV, positive predictive value; PSAD, tPSA density; S23PSA, α2,3-sialylated prostate-specific antigen ratio; S23PSAD, S23PSA density; tPSA, total PSA.

[a]Mann–Whitney U test.

[b]χ^2 test.

3.3 | Use of S23PSAD improves the rate of avoidable SBx

The DCAs predicting PC in the retrospective SBx cohort revealed that S23PSA and S23PSAD significantly contribute to the prediction of HGPC (over the usage of traditional factors of tPSA and DRE) from 10% to 20% and ≥21% risk threshold, respectively, which entails the defined range of plausible threshold probabilities (10%–40%). For example, at the 30% risk threshold, the risk of 30% is an odds of 3:7, the doctor says "missing a PC is 2.3 times worse than doing an unnecessary biopsy." This can be interpreted as the "number-needed-to-test," that is, 30% is a number-needed-to-test of 30. At the 30% risk threshold, the rate of avoidable SBx without missing PC or HGPC using S23PSA (9% or 17%) and S23PSAD (5% or 21%) compared with using of tPSA and DRE (0% or 0%), tPSA, DRE and F/T PSA (3% or 4%), and tPSA, DRE and PSAD (4% or 17%) (Figure 3E).

The DCAs predicting PC in the retrospective SBx subcohort of patients with tPSA levels ranging from 4 to 10 ng/ml revealed that S23PSA and S23PSAD significantly contribute to the prediction of HGPC (over the use of traditional factors of tPSA and DRE) from 10% to 22% and more than or equal to 23% risk threshold, respectively, which is well within the defined range of plausible threshold probabilities (10%–40%). For example, at the 30% risk threshold, the rate of avoidable SBx without missing PC or HGPC using tPSA, DRE, and S23PSA (8% or 14%) and tPSA, DRE, and S23PSAD (5% or 21%) was significantly higher than using tPSA and DRE (0% or –2%), tPSA, DRE, and F/T PSA (3% or 11%), and tPSA, DRE, and PSAD (3% or 16%) (Figure 3F). Collectively, these results suggest that the use of S23PSA or S23PSAD can avoid unnecessary SBx.

3.4 | Diagnostic performance of S23PSA and S23PSAD as compared to mpMRI

We further investigated the clinical impact of S23PSA and S23PSAD in comparison with mpMRI in the prospective observational MRI–TBx cohort. The characteristics of the 98 patients in the MRI–TBx cohort are shown in Table 3. Among the 56 patients with PC, six were classified as GG1, and the remaining 50 patients with HGPC were classified as GG2 (17, 30.4%), GG3 (5, 8.9%), GG4 (13, 23.2%), and GG5 (15, 26.8%). No significant differences in age, DRE status, and tPSA level were found between the two groups.

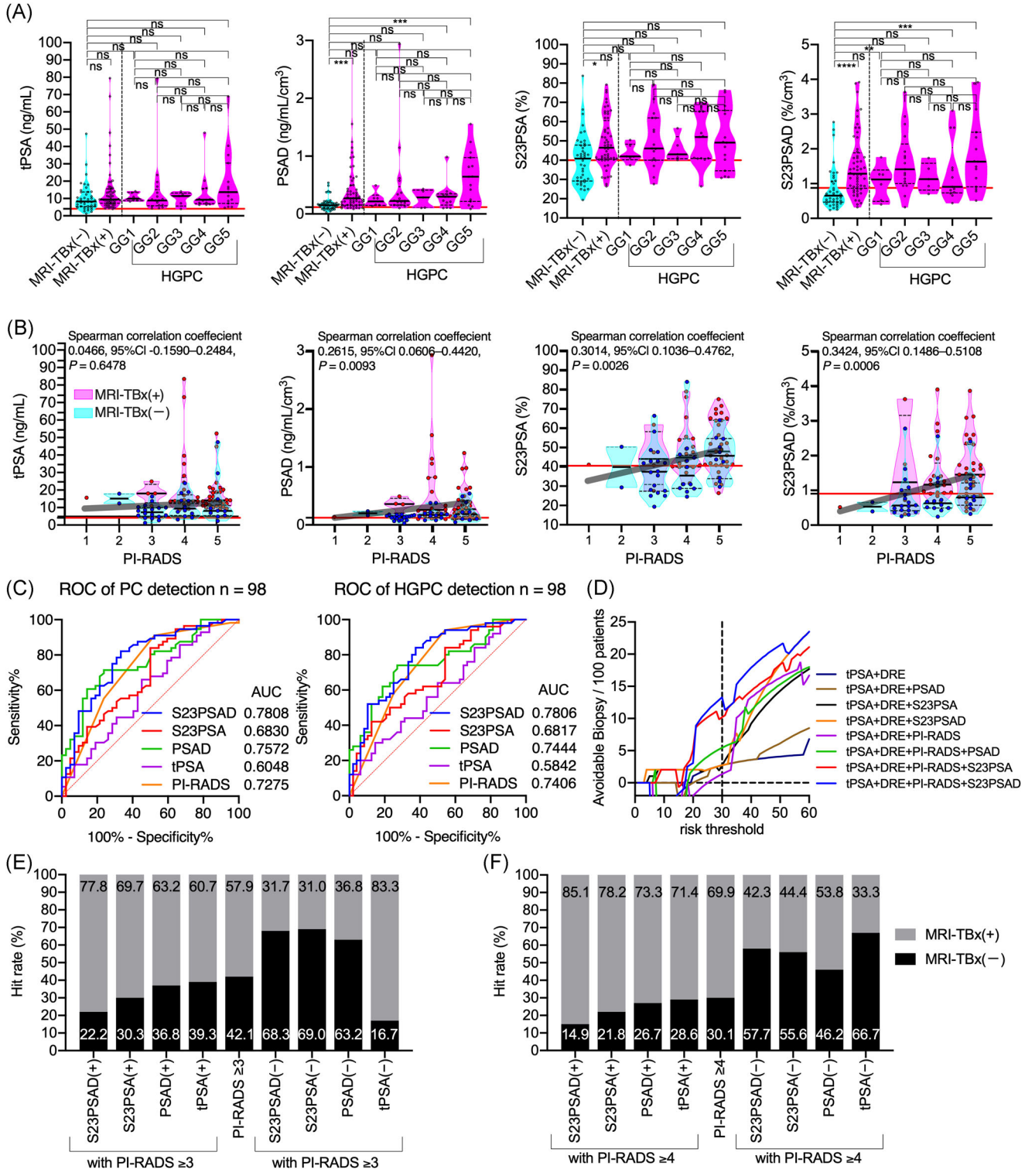

FIGURE 4 (See caption on next page)

However, significant differences in prostate volume, PSAD, S23PSA, and S23PSAD were found between MRI–TBx(−) and MRI–TBx(+) men ($p = 0.0005$, $p = 0.0001$, $p = 0.0150$, and $p < 0.0001$, respectively) (Figure 4A and Table 3). S23PSAD (Spearman correlation coefficient, 0.3424; 95% CI, 0.1486–0.5108; $p = 0.0006$), S23PSA (0.3014; 95% CI, 0.1036–0.4762; $p = 0.0026$), and PSAD (0.2615; 95% CI, 0.0606–0.4420; $p = 0.0093$) weakly correlated with PI-RADS score, whereas tPSA (0.0466; 95% CI, − 0.1590 to 0.2484; $p = 0.6478$) did not correlate with the PI-RADS score (Figure 4B).

The AUC of S23PSAD for detection of PC (0.7808; 95% CI, 0.6872–0.8744) was higher than that of tPSA (0.6048; 95% CI, 0.4906–0.7190) ($p = 0.0393$), PSAD (0.7572; 95% CI, 0.6624–0.8521) ($p = 0.6546$), S23PSA (0.6830; 95% CI, 0.5753–0.7907) ($p = 0.0148$), and PI-RADS (0.7275; 95% CI, 0.6232–0.8317) ($p = .3991$) (Figure 4C, Table 2). The AUC of S23PSAD for predicting HGPC (0.7806; 95% CI, 0.6894–0.8718) was higher than that of tPSA (0.5842; 95% CI, 0.4714–0.6969) ($p = 0.0146$), PSAD (0.7444; 95% CI, 0.6465–0.8422) ($p = 0.4356$), S23PSA (0.6817; 95% CI, 0.5766–0.7867) ($p = 0.0287$), and PI-RADS (0.7406; 95% CI, 0.6412–0.8400) ($p = 0.4859$) (Figure 4C, Table 4).

When applying a cutoff value of 90% sensitivity for each assay as determined in the retrospective SBx cohort (Table 2), the DCA predicting PC in the prospective MRI–TBx cohort revealed that PI-RADS + S23PSAD had the largest net benefit for predicting PC at ≥20% risk threshold, which is well within the range of plausible threshold probabilities (10%–40%). For example, at the 30% risk threshold, the rate of avoidable MRI–TBx without missing PC using PI-RADS + S23PSAD amounted to 13%, a significant increase over tPSA and DRE (3%), tPSA, DRE and PI-RADS (1%), tPSA, DRE, PI-RADS and PSAD (5%), and tPSA, DRE, PI-RADS, and S23PSA (10%) (Figure 4D). These results show that combining S23PSAD and PI-RADS improves the avoidance rate of unnecessary prostate biopsies.

When applying the cutoff value of each assay as determined in the retrospective SBx cohort (Table 2), 77.8% (42/54 cases) had an S23PSAD(+) (≥0.8750%/cm^3) with PI-RADS ≥ 3 in MRI–TBx(+) men, which was higher than the detection rate of S23PSA(+) (≥39.95%) with PI-RADS ≥ 3 (69.7%, 46/66), PSAD(+) (≥0.1165 ng/mlcm^3) with PI-RADS ≥ 3 (63.2%, 48/76), and tPSA(+) with PI-RADS ≥ 3 (60.7%, 54/89) (Figure 4E). Conversely, of the 41 cases, 28 (68.3%) had an S23PSAD (−) (<0.8750%/cm^3) with PI-RADS ≥ 3 in MRI–TBx(−) men, which was higher than the detection rate of S23PSA(−) (<39.95%) with PI-RADS ≥ 3 (69.0%, 20/29), and PSAD(−) (<0.1165 ng/mlcm^3) with PI-RADS ≥ 3 (63.2%, 12/19) (Figure 4E). Of the 47 cases, 40 (85.1%) had an S23PSAD(+) with PI-RADS ≥ 4 in MRI–TBx(+) men, which was higher than the detection rate of S23PSA(+) with PI-RADS ≥ 4 (78.2%, 43/55), PSAD(+) with PI-RADS ≥ 4 (72.4%, 44/60), and tPSA(+) with PI-RADS ≥ 4 (71.4%, 50/70) (Figure 4F). Of the 26 cases, 15 (57.7%) had an S23PSAD(−) with PI-RADS ≥ 4 in MRI–TBx (−) men, which was higher than the detection rate of S23PSA(−) with PI-RADS ≥ 4 (55.6%, 10/18), and PSAD(−) with PI-RADS ≥ 4 (46.2%, 6/13) (Figure 4F).

Among the 98 patients in the MRI–TBx cohort, 79 (≤75 years old and tPSA of ≤50 ng/ml) were available to use European Randomized Study of Screening for Prostate cancer risk calculators (ERSPC RCs). The diagnostic performance comparing ERSPC RCs and S23PSA assay is shown in supplementary files.

4 | DISCUSSION

Aberrantly glycosylated PSA (e.g., S23PSA and LacdiNAc-PSA) in serum is significantly increased in PC,[10–14,20–22] and in particular in high-grade GG ≥ 2 PC.[11,23] The amount of LacdiNAc-glycan on PC tissue is positively correlated with higher GG and is an independent risk factor for PSA recurrence.[23] LacdiNAc-PSA/tPSA ratios and the expression of LacdiNAc-glycan synthesis-related glycosyltransferase are increased in higher Gp tissues,[9] suggesting that LacdiNAc-glycan synthesis is increased in aggressive tumors. Our results here show that α2,6-sialylation-related *ST6GAL1* gene expression was significantly decreased in higher Gp tissues, whereas α2,3-sialylation-related *ST3GAL3*, *4*, *6* gene and sialidase *NEU1–4* gene expressions did not change, leading to an increase in the ratio of α2,3-sialylated *N*-glycan on PSA (S23PSA) in HGPC. Thus, the synthesis of S23PSA mainly characterizes HGPC tissue. Although the biological function of

FIGURE 4 Serum levels and ROC curve analysis of S23PSA, S23PSAD, tPSA, and PSAD in the prospective MRI–TBx cohort. (A) *Violin plot* of each test in the prospective MRI–TBx cohort. The MRI–TBx (+) group was classified as GG 1, and the HGPC group includes GG2, GG3, GG4, and GG5. Multiple group differences were analyzed using the Kruskal–Wallis test for non-normally distributed models. *ns* not significant, $^*p < 0.05$, $^{**}p < 0.005$, $^{***}p < 0.0005$. (B) The correlation between each assay level and the PI-RADS score in the MRI–TBx cohort. The *dashed black lines* outline the IQR of each test value. The *solid bold black line* represents the median value of each test. The *solid bold red line* represents the cutoff value defined by the retrospective SBx cohort. The *solid bold gray line* represents the linear regression correlation curve. The *light blue violin plot* represents MRI–TBx(−) patients, and the *pink violin plot* represents MRI–TBx(+) patients. (C) ROC curves of PC and HGPC prediction accuracy of tPSA, PSAD, S23PSA, and S23PSAD in the MRI–TBx cohort. (D) DCA showing net benefit for performing a biopsy in men at risk of PC in the MRI–TBx cohort. The number of avoidable biopsies per 100 patients without missing PC in the MRI–TBx cohort. (E) and (F) MRI–TBx(+) or MRI–TBx(−) hit rate of each assay positively combined with PI-RADS ≥ 3 cases (E) and each assay positively combined with PI-RADS ≥ 4 case (F). DCA, decision curve analyses; MRI, magnetic resonance imaging; PI-RADS, Prostate Imaging Reporting and Data System Version 2; PSAD, PSA density tPSA normalized by prostate volume; PSA, prostate-specific antigen; ROC, receiver operating characteristic curve; tPSA, total PSA [Color figure can be viewed at wileyonlinelibrary.com]

TABLE 4 Specificity at defined cutoff value of each assay in prospective MRI–TBx cohort

PC detection	tPSA	PSAD	S23PSA	S23PSAD	PI-RADS	
Cut-off	>4.025 ng/ml	>0.1165 ng/ml/cm^3	>39.95%	>0.8750%/cm^3	≥4	
AUC (95% CI)	0.6048 (0.4906–0.7190)	0.7572 (0.6624–0.8521)	0.6830 (0.5753–0.7907)	0.7808 (0.6872–0.8744)	0.7275 (0.6232–0.8317)	
p (vs. S23PSAD)	0.0393	0.6546	0.0148		0.3991	
Sensitivity, %	98.2	87.5	83.9	75.0	91.1	
Specificity, %	11.9	28.6	50.0	71.4	47.6	
PPV, %	59.8	62.0	69.1	77.8	69.9	
NPV, %	83.3	63.2	70.0	68.2	80.0	
FPR, %	88.1	71.4	50.0	28.6	52.4	
FNR, %	1.8	12.5	16.1	25.0	8.9	
HGPC detection	tPSA	PSAD	S23PSA	S23PSAD	PI-RADS	
Cut-off	>4.275 ng/ml	>0.1295 ng/ml/cm^3	>41.45%	>0.9770%/cm^3	≥4	
AUC (95% CI)	0.5842 (0.4714–0.6969)	0.7444 (0.6465–0.8422)	0.6817 (0.5766–0.7867)	0.7806 (0.6894–0.8718)	0.7406 (0.6412–0.8400)	
p (vs. S23PSAD)	0.0146	0.4356	0.0287		0.4859	
Sensitivity, %	98.0	83.7	63.3	65.3	93.9	
Specificity, %	14.3	30.6	49.0	67.3	44.9	
PPV, %	53.3	54.7	55.4	66.7	63.0	
NPV, %	87.5	65.2	57.1	66.0	88.0	
FPR, %	85.7	69.4	51.0	32.7	55.1	
FNR, %	2.0	16.3	36.7	34.7	6.1	
Specificity at defined cutoff value of each assay in prospective MRI–TBx cohort (≤75 years old and tPSA ≤50 ng/ml)						
PC detection	tPSA	PSAD	S23PSA	S23PSAD	PI-RADS	ERSPC RCs
Cut-off	>4.025 ng/ml	>0.1165 ng/ml/cm^3	>39.95%	>0.8750%/cm^3	≥4	>20%
AUC (95% CI)	0.5058 (0.3757–0.6359)	0.7177 (0.6026–0.8328)	0.7255 (0.6147–0.8362)	0.8194 (0.7279–0.9110)	0.7661 (0.6618–0.8705)	0.8737 (0.7995–0.9480)
p (vs. ERSPC RCs)	0.0001	0.0678	0.1124	0.6509	0.0069	
Sensitivity, %	97.6	87.8	85.4	75.6	92.7	97.6
Specificity, %	13.2	28.9	50.0	73.7	47.4	47.4
PPV, %	54.8	57.1	64.8	75.6	65.5	66.7
NPV, %	83.3	68.8	76.0	73.7	85.7	94.7
FPR, %	86.8	71.1	50.0	26.3	52.6	52.6
FNR, %	2.4	12.2	14.6	24.4	7.3	2.4
HGPC detection	tPSA	PSAD	S23PSA	S23PSAD	PI-RADS	ERSPC RCs
Cut-off	>4.275 ng/ml	>0.1295 ng/ml/cm^3	>41.45%	>0.9770%/cm^3	≥4	>20%
AUC (95% CI)	0.5353 (0.4063–0.6643)	0.7237 (0.6121–0.8353)	0.7234 (0.6127–0.8341)	0.8071 (0.7100–0.9042)	0.7465 (0.6355–0.8575)	0.8338 (0.7445–0.9230)
p (vs. ERSPC RCs)	<0.0001	0.0127	0.0724	0.4028	0.0035	
Sensitivity, %	97.1	82.9	68.6	71.4	97.1	100.0
Specificity, %	15.9	31.8	50.0	68.2	45.5	43.2
PPV, %	47.9	49.2	52.2	64.1	58.6	58.3
NPV, %	87.5	70.0	66.7	75.0	95.2	100.0

TABLE 4 (Continued)

PC detection	tPSA	PSAD	S23PSA	S23PSAD	PI-RADS	
FPR, %	84.1	68.2	50.0	31.8	54.5	56.8
FNR, %	2.9	17.1	31.4	28.6	2.9	0.0

Abbreviations: AUC, area under the receiver operating characteristics curve; ERSPC RCs, European Randomized Study of Screening for Prostate cancer risk calculators; F/T PSA, free PSA/tPSA; FNR, false-negative rate; FPR, false-positive rate; HGPC, high-grade PC; MRI, magnetic resonance imaging; NPV, negative predictive value; PC, prostate cancer; PI-RADS, Prostate Imaging Reporting and Data System; PPV, positive predictive value; PSAD, tPSA density; S23PSA, α2,3-sialylated prostate-specific antigen ratio; S23PSAD, S23PSA density; tPSA, total PSA.

aberrant glycosylation on PC tissue remains unclear, aberrant glycosylated PSA may be a useful biomarker for HGPC.

Triggered by tPSA levels ≥4.0 ng/ml and/or abnormal DRE, millions of TRUS-guided SBx are performed every year. These are costly and often associate with pain, anxiety, and complications.[24,25] Consequently, the tPSA-based PC screening strategy now includes the use of mpMRI to target HGPC (GG ≥ 2), retaining the potential for continued mortality reduction but avoiding harm from overdetection of indolent PC. A Cochrane systematic review including 18 studies has shown a high negative predictive value for detecting HGPC (91%) and low risk of missing HGPC in biopsy-naïve men who have a negative mpMRI (9%).[26] Another systematic review which included 48 studies showed that the median negative predictive value of mpMRI for detecting PC and clinically significant PC is 82.4% (interquartile range (IQR), 69.0%–92.4%) and 88.1% (IQR, 85.7%–92.3%) while noting a high variability in the reported performance of mpMRI to detect PC between studies.[27] A single-center prospective study assessing variability in mpMRI reporting across radiologists of varying experience in routine clinical care has shown that 13%–60% of clinically significant PC would be missed if a biopsy was only performed in men with PI-RADS ≥ 3.[28] To improve the detection of clinically significant PC, several potent biomarkers were suggested to be combined with mpMRI.[29,30] The SelectMDx score associates with PI-RADS and its performance to predict the mpMRI outcome (AUC, 0.83) is significantly higher than PSA (AUC, 0.66) and PCA3 (AUC, 0.65).[29] Adding 4Kscore to mpMRI improves the predictive performance for detecting HGPC (AUC, 0.82).[30] These results suggest that SelectMDx or 4Kscore could guide clinicians in selecting patients for further mpMRI. Several biomarkers (PHI, 4KScore, PCA3, MiPS, SelectMDx, and EPI) and MRI imaging have demonstrated promising results for predicting HGPC.[31,32] Our retrospective SBx cohort study found that the AUCs of S23PSA and S23PSAD for detecting both PC and HGPC were superior to those of tPSA, F/T PSA, and PSAD. Consequently, S23PSAD or S23PSA perform better than PSA or PSAD. Here we report for the first time that the diagnostic accuracy of mpMRI can be significantly improved by the addition of S23PSA and/or S23PSAD. S23PSAD level positively correlated with the PI-RADS score and the addition of S23PSAD using a cutoff value of ≥0.8750%/cm^3 to cases with PI-RADS ≥ 3 or ≥4 cases improved the detection rate of PC. These results and the DCA show that the inclusion of S23PSAD + PI-RADS can further reduce unnecessary prostate biopsies.

The limitations of this study include its retrospective nature, the absence of family history and MRI before biopsy in the SBx cohort and the relatively small sample size in the single-center prospective MRI–TBx cohort. The latter prevented us from drawing further conclusions regarding the added value of S23PSAD in detecting HGPC when combined with mpMRI. Further larger prospective clinical trials using S23PSAD + PI-RADS and comparison to the performance of other commercially available biomarkers would resolve the cost-effectiveness and clinical significance of the S23PSA assay.

In conclusion, we show that PC-diagnostic performance of S23PSAD is superior to conventional strategies and that the combination of S23PSAD with mpMRI improves the detection rate of PC and thus may result in avoiding unnecessary biopsies.

ACKNOWLEDGMENTS

The authors thank Yukie Nishizawa, Mitsuharu Miyadate, and Satomi Sakamoto, technical assistants of Hirosaki University, for their invaluable help with the sample collection. This study was supported by the Japan Society for the Promotion of Science (JSPS) KAKENHI (grant nos. 15K15579 and 15H02563) and also supported by Sakurai Memorial Medical Research Foundation.

CONFLICT OF INTERESTS

The authors declare that there are no conflict of interests.

AUTHOR CONTRIBUTIONS

Study concept and design: Tohru Yoneyama, Hayato Yamamoto, and Chikara Ohyama. *Acquisition of data*: Tohru Yoneyama, Hayato Yamamoto, Mihoko Sutoh Yoneyama, Yuki Tobisawa, Shingo Hatakeyama, Takuma Narita, Hirotake Kodama, Masaki Momota, Masaki Ito, Fumiyasu Tsushima, Shintaro Narita, Koji Mitsuzuka, Takahiro Yoneyama, Yasuhiro Hashimoto, Wilhelmina Duivenvoorden, Jehonathan H. Pinthus, Shingo Kakeda, Akihiro Ito, Norihiko Tsuchiya, Tomonori Habuchi, and Chikara Ohyama. *Analysis and interpretation of data*: Tohru Yoneyama and Hayato Yamamoto. Drafting of the manuscript: Tohru Yoneyama, Hayato Yamamoto, Mihoko Sutoh Yoneyama, Yuki Tobisawa, Shingo Hatakeyama, Takuma Narita, Hirotake Kodama, Masaki Momota, Masaki Ito, Fumiyasu Tsushima, Shintaro Narita, Koji Mitsuzuka, Takahiro Yoneyama, Yasuhiro Hashimoto, Wilhelmina Duivenvoorden, Jehonathan H. Pinthus, Shingo Kakeda, Akihiro Ito,

Norihiko Tsuchiya, Tomonori Habuchi, and Chikara Ohyama. *Critical revision of the manuscript for important intellectual content*: Tohru Yoneyama, Hayato Yamamoto, Wilhelmina Duivenvoorden, Jehonathan H. Pinthus, and Chikara Ohyama. *Statistical analysis*: Tohru Yoneyama and Hayato Yamamoto. *Obtaining funding*: Tohru Yoneyama and Chikara Ohyama. *Administrative, technical, or material support*: Tohru Yoneyama and Hayato Yamamoto. Supervision: Tohru Yoneyama and Chikara Ohyama. *Others*: None.

DATA AVAILABILITY STATEMENT

All data needed to evaluate the conclusions in the paper are present in the paper and/or the Supplementary Materials. Additional data related to this paper may be requested from the authors.

ENDNOTE

† The study on the clinical significance of S23PSA test; approval number, 2019–055, https://www.med.hirosaki-u.ac.jp/hospital/outline/resarch/resarch.html).

ORCID

Tohru Yoneyama https://orcid.org/0000-0002-1098-407X
Hayato Yamamoto https://orcid.org/0000-0002-4557-0619
Yuki Tobisawa https://orcid.org/0000-0001-8026-9541
Shingo Hatakeyama https://orcid.org/0000-0002-0026-4079
Takuma Narita https://orcid.org/0000-0003-2572-3590
Hirotake Kodama https://orcid.org/0000-0002-5071-5149
Shintaro Narita https://orcid.org/0000-0003-2988-1860
Fumiyasu Tsushima https://orcid.org/0000-0003-1806-8233
Koji Mitsuzuka https://orcid.org/0000-0002-5017-5568
Takahiro Yoneyama https://orcid.org/0000-0003-1061-827X
Yasuhiro Hashimoto https://orcid.org/0000-0003-0967-6835
Wilhelmina Duivenvoorden https://orcid.org/0000-0003-3439-9163
Jehonathan H. Pinthus https://orcid.org/0000-0001-6980-7601
Shingo Kakeda https://orcid.org/0000-0002-0521-9728
Akihiro Ito https://orcid.org/0000-0001-7224-1100
Norihiko Tsuchiya https://orcid.org/0000-0003-4242-2618
Tomonori Habuchi https://orcid.org/0000-0003-0998-4432
Chikara Ohyama https://orcid.org/0000-0003-1550-8379

REFERENCES

1. Klotz L. Prostate cancer overdiagnosis and overtreatment. *Curr Opin Endocrinol Diabetes Obes*. 2013;20:204-209.
2. Kim EH, Andriole GL. Prostate-specific antigen-based screening: controversy and guidelines. *BMC Med*. 2015;13:61.
3. Kretschmer A, Tilki D. Biomarkers in prostate cancer: current clinical utility and future perspectives. *Crit Rev Oncol Hematol*. 2017;120:180-193.
4. Loeb S, Sanda MG, Broyles DL, et al. The prostate health index selectively identifies clinically significant prostate cancer. *J Urol*. 2015;193:1163-1169.
5. Nordstrom T, Vickers A, Assel M, Lilja H, Gronberg H, Eklund M. Comparison between the four-kallikrein Panel and Prostate Health Index for predicting prostate cancer. *Eur Urol*. 2015;68(1):139-146. https://www.sciencedirect.com/science/article/abs/pii/S0302283814007520?via%3Dihub
6. Leyten GH, Hessels D, Smit FP, et al. Identification of a candidate gene panel for the early diagnosis of prostate cancer. *Clin Cancer Res*. 2015;21:3061-3070.
7. Tomlins SA, Day JR, Lonigro RJ, et al. Urine TMPRSS2:ERG plus PCA3 for individualized prostate cancer risk assessment. *Eur Urol*. 2016;70:45-53.
8. McKiernan J, Donovan MJ, O'Neill V, et al. A novel urine exosome gene expression assay to predict high-grade prostate cancer at initial biopsy. *JAMA Oncol*. 2016;2:882-889.
9. Yoneyama T, Tobisawa Y, Kaneko T, et al. Clinical significance of the LacdiNAc-glycosylated prostate-specific antigen assay for prostate cancer detection. *Cancer Sci*. 2019;110:2573-2589.
10. Ishikawa T, Yoneyama T, Tobisawa Y, et al. An automated micro-total immunoassay system for measuring cancer-associated alpha2,3-linked sialyl N-glycan-carrying prostate-specific antigen may improve the accuracy of prostate cancer diagnosis. *Int J Mol Sci*. 2017;18:18.
11. Inoue T, Kaneko T, Muramatsu S, et al. LacdiNAc-glycosylated prostate-specific antigen density is a potential biomarker of prostate cancer. *Clin Genitourin Cancer*. 2020;18:e28-e36.
12. Haga Y, Uemura M, Baba S, et al. Identification of multisialylated LacdiNAc structures as highly prostate cancer specific glycan signatures on PSA. *Anal Chem*. 2019;91:2247-2254.
13. Tajiri M, Ohyama C, Wada Y. Oligosaccharide profiles of the prostate specific antigen in free and complexed forms from the prostate cancer patient serum and in seminal plasma: a glycopeptide approach. *Glycobiology*. 2008;18:2-8.
14. Ohyama C, Hosono M, Nitta K, et al. Carbohydrate structure and differential binding of prostate specific antigen to Maackia amurensis lectin between prostate cancer and benign prostate hypertrophy. *Glycobiology*. 2004;14:671-679.
15. Weinreb JC, Barentsz JO, Choyke PL, et al. PI-RADS prostate imaging - Reporting and Data System: 2015, Version 2. *Eur Urol*. 2016;69:16-40.
16. Humphrey PA, Moch H, Cubilla AL, Ulbright TM, Reuter VE. The 2016 WHO Classification of tumours of the urinary system and male genital organs-part b: prostate and bladder tumours. *Eur Urol*. 2016;70:106-119.
17. Van Calster B, Wynants L, Verbeek JFM, et al. Reporting and interpreting decision curve analysis: a guide for investigators. *Eur Urol*. 2018;74:796-804.
18. Mehta KA, Patel KA, Pandya SJ, Patel PS. Aberrant sialylation plays a significant role in oral squamous cell carcinoma progression. *J Oral Pathol Med*. 2020;49:253-259.
19. Lee WL, Wang PH. Aberrant sialylation in ovarian cancers. *J Chin Med Assoc*. 2020;83:337-344.
20. Hirano K, Matsuda A, Shirai T, Furukawa K. Expression of LacdiNAc groups on N-glycans among human tumors is complex. *BioMed Res Int*. 2014;2014:981627.
21. Fukushima K, Satoh T, Baba S, Yamashita K. alpha1,2-Fucosylated and beta-N-acetylgalactosaminylated prostate-specific antigen as an efficient marker of prostatic cancer. *Glycobiology*. 2010;20:452-460.
22. Yoneyama T, Ohyama C, Hatakeyama S, et al. Measurement of aberrant glycosylation of prostate specific antigen can improve specificity in early detection of prostate cancer. *Biochem Biophys Res Commun*. 2014;448:390-396.
23. Hagiwara K, Tobisawa Y, Kaya T, et al. Wisteria floribunda agglutinin and its reactive-glycan-carrying prostate-specific antigen as a novel diagnostic and prognostic marker of prostate cancer. *Int J Mol Sci*. 2017;18:18.
24. Borghesi M, Ahmed H, Nam R, et al. Complications after systematic, random, and image-guided prostate biopsy. *Eur Urol*. 2017;71:353-365.

25. Wade J, Rosario DJ, Macefield RC, et al. Psychological impact of prostate biopsy: physical symptoms, anxiety, and depression. *J Clin Oncol*. 2013;31:4235-4241.
26. Drost FH, Osses DF, Nieboer D, et al. Prostate MRI, with or without MRI-targeted biopsy, and systematic biopsy for detecting prostate cancer. *Cochrane Database Syst Rev*. 2019;4:CD012663.
27. Moldovan PC, Van den Broeck T, Sylvester R, et al. What is the negative predictive value of multiparametric magnetic resonance imaging in excluding prostate cancer at biopsy? A systematic review and meta-analysis from the European Association of Urology Prostate Cancer Guidelines Panel. *Eur Urol*. 2017;72:250-266.
28. Sonn GA, Fan RE, Ghanouni P, et al. Prostate magnetic resonance imaging interpretation varies substantially across radiologists. *Eur Urol Focus*. 2019;5:592-599.
29. Hendriks RJ, van der Leest MMG, Dijkstra S, et al. A urinary biomarker-based risk score correlates with multiparametric MRI for prostate cancer detection. *Prostate*. 2017;77:1401-1407.
30. Punnen S, Nahar B, Soodana-Prakash N, et al. Optimizing patient's selection for prostate biopsy: a single institution experience with multi-parametric MRI and the 4Kscore test for the detection of aggressive prostate cancer. *PLoS One*. 2018;13:e0201384.
31. Haider MA, Yao X, Loblaw A, Finelli A. Multiparametric magnetic resonance imaging in the diagnosis of prostate cancer: a systematic review. *Clin Oncol* 2016;28:550-567.
32. Hendriks RJ, van Oort IM, Schalken JA. Blood-based and urinary prostate cancer biomarkers: a review and comparison of novel biomarkers for detection and treatment decisions. *Prostate Cancer Prostatic Dis*. 2017;20:12-19.

SUPPORTING INFORMATION

Additional supporting information may be found in the online version of the article at the publisher's website.

How to cite this article: Yoneyama T, Yamamoto H, Yoneyama MS, et al. Characteristics of α2,3-sialyl *N*-glycosylated PSA as a biomarker for clinically significant prostate cancer in men with elevated PSA level. *The Prostate*. 2021;81:1411-1427. https://doi.org/10.1002/pros.24239